The nanomechanical fingerprint of colorectal-derived peritoneal metastasis

Ewelina Lorenc[1], Luca Varinelli[2], Matteo Chighizola[1], Silvia Brich[3], Federica Pisati[4], Marcello Guaglio[5], Dario Baratti[5], Marcello Deraco[5], Manuela Gariboldi[2, *], Alessandro Podesta[1,*]

[1] Dipartimento di Fisica "Aldo Pontremoli" and CIMaINa, Università degli Studi di Milano, via G. Celoria 16, 20133, Milano, Italy.

[2] Department of Research, Fondazione IRCCS Istituto Nazionale Tumori, via G. Venezian 1, 20133 Milano, Italy.

[3] Department of Pathology and Laboratory Medicine, Fondazione IRCCS Istituto Nazionale dei Tumori, via G. Venezian 1, 20133 Milano, Italy.

[4] Cogentech Ltd. Benefit corporation with a sole shareholder, via Adamello 16, 20139 Milan, Italy.

[5] Peritoneal Surface Malignancies Unit, Colon and Rectal Surgery, Fondazione IRCCS Istituto Nazionale Tumori, via G. Venezian 1, 20133, Milano, Italy.

*Corresponding authors. E-mail: alessandro.podesta@mi.infn.it, Manuela.Gariboldi@istitutotumori.mi.it

Abstract

Peritoneal metastases (PM) are one of the most common routes of dissemination for colorectal cancer (CRC) and remain a lethal disease with a poor prognosis. The compositional, mechanical and structural properties of the extracellular matrix (ECM) play an important role in cancer development; studying how these properties change during the progression of the disease is crucial to understand metastasis from colorectal cancer.

The elastic properties of human derived ECMs of normal and neoplastic PM in the different pathological conditions were studied by atomic force microscopy (AFM) and the results were correlated to patients' clinical data and to the results of immuno-histological assays targeting different biomarkers of the CRC tumor and its metastases.

Our results show that the progression of peritoneal metastasis is accompanied by stiffening of ECM as a common feature; spatially resolved mechanical analysis highlighted significant spatial heterogeneity of the elastic properties of both normal and neoplastic ECMs, which show significant overlap in the two conditions. On the micrometre scale, ECMs that are considered as normal according to the anatomopathological classification possess stiffer spatial domains, which are typically associated with cancer associated fibroblasts (CAF) activity and tumor development in neoplastic matrices; on the other hand, softer regions are found in neoplastic ECMs on the same scales Our results support the hypothesis that local changes (stiffening) of the normal ECM can set the ground for the grow and spread of the tumor from invading metastatic cells.

Mechanical changes correlate well with the presence of CAF and increase in collagen deposition, which are well known markers of cancer progression. Furthermore, we have found interesting correlations between the mechanical properties of the ECM and patients' clinical data like age, sex and protein mutations.

Overall, our findings suggest that the mechanical phenotyping of the ECM of CRC patients has a potential for detecting tumor development and discriminate specific cancer oncogenes.

Keywords: *colorectal carcinoma, peritoneal metastasis, extracellular matrix (ECM), nanomechanics, atomic force microscopy (AFM).*

Introduction

Peritoneal Metastasis (PM) affects about one out of every four patients with colorectal cancer (CRC) [1]. PM is characterized by several steps where tumor cells disseminate from the primary tumor to the peritoneal cavity [2], through a process also known as peritoneal metastatic cascade [2,3]. To colonize the peritoneum, the neoplastic cells have to be able to infiltrate the extracellular matrix (ECM), starting from the detachment from primary tumour, attach to sub-mesothelial connective tissue and receive a favourable host response[2].

ECM is an essential, acellular element in tissue microenvironment, which plays a crucial role in several processes like tissue homeostasis, it determines the three-dimensional (3D) structure of the tissue [4], provides mechanical and biochemical support[5–7]playing a major role in cell-cell and cell-matrix communication [6–8], cell migration[8,9]. Because of its crucial role in many biological aspects, it is also extremely relevant in cancer progression, as demonstrated in several works in recent years [7,10–15]

The extra-cellular microenvironment is composed of water, various fibrous proteins (collagens, elastins, laminins, fibronectins), proteoglycans, glycoproteins, and polysaccharides[1,6,8]. Since every organ plays different role in the human body, the ECM of the specific tissue has unique composition and topology, which results in developing the biochemical and mechanical properties of each organ and tissue [4–6,16,17]. The ECM can be consider a dynamic element of the tissue, since it undergoes several changes in its composition and rearrangements of particular own components, through covalent and non-covalent modifications, which are associated with cells activity in tissue development [8,16], severe diseases and cancer progression [1,4,8,18]. Both mechanical and biochemical changes in ECM are regulated by growth factors, hormones, cytokines and metalloproteinases (MMP)[5]. The ECM's elastic properties, together with activity of specific biochemical factors, play a key role in tissue homeostasis, cells fate, cells adhesion, migration, cell cycle progression, differentiation and actin cytoskeletal reorganization and contractility[16].

During cancer progression, the ECM undergoes many structural and biochemical changes, such as increase of collagen deposition and fiber cross-linkingchanges in gene expression (e.g. Lysil oxidase (LOX) and metalloproteinase (MMP) overexpression) [5,6,8,16–18]. As one of many outcomes of tumour development, the stiffening of ECM is associated with high malignancy/aggressiveness and bad prognosis[14,19–21]. The stiffening of the ECM, occurring also during tissue aging as a natural phenomenon[6], can be observed in pre-malignant and malignant tissues[5,16], which leads to enhanced therapy resistance in most of the tumors [5].

The main events responsible for ECM stiffening are deposition and remodelling of collagen and elastin fibers, which are caused by LOX and transglutaminase activity[6]. Cancer associated fibroblasts (CAFs) are critical in the progression of metastatic disease; they can originate from different cell types, including resident fibroblasts and mesothelial cells, which undergo a mesothelial-to-mesenchymal transition (MMT)[1,22]. CAFs oversee producing ECM proteins such as collagen, fibronectin, and a variety of others, as well as proteases and other enzymes involved in post-transcriptional modification of ECM proteins[22–24].

Since one of the signs of cancer progression are CAF activation and collagen deposition, which lead to overall increase of ECM elastic modulus (stiffening), the early detection of ECM stiffening at the cellular scale could allow to spot first signs of tumor development and monitor cancer progression at early stages. Moreover, a better understanding of the ECM stiffening process and the associated cell-ECM interplay could help developing more efficient therapeutic strategies in prevention or treatment of cancer diseases.

Atomic force microscopy is a powerful and versatile tool to study biological samples at the nano- and microscale [25–27], for the quantitative investigation of their morphological and mechanical properties [28,29][29]. In particular, the mechanical properties of cells, ECMs and tissues can be characterized by AFM [4,7,30–34] and identified as a unique mechanical fingerprint of cancer progression [35,36].

Our work was motivated by the idea that AFM study of nanomechanical properties of cells, ECMs and tissues can provide an important contribution in cancer research, when complemented by immunostaining and other biochemical assays, and the results correlated

with clinical metadata (anatomopathological classification of the disease, age, sex, previous treatments, etc.). We have therefore studied the changes in the mechanical properties of the ECM in patients affected by peritoneal metastasis deriving from colorectal cancer. In particular, we have characterized the Young's modulus of elasticity of ECM specimens by means of indentation measurements performed by AFM[28]. We have correlated the results of the nanomechanical analysis with the presence of CAF and collagen organisation in the ECM samples, to obtain insights into the physicochemical differences between normal and neoplastic ECMs.

Materials and methods

Sample preparation

In this work, we studied ECMs obtained from tissues of human-derived peritoneum. All the 14 patients were diagnosed with PM from CRC (more detailed information are in table 1). The study was approved by the Institutional review board (134/13; I249/19) and was conducted in accordance with the Declaration of Helsinki, 2009. Written informed consent was acquired. The samples of peritoneal tissue were collected during surgical resection at the Peritoneal Malignaces Unit of Fondazione IRCCS Istituto Nazionale Tumori.

Sample collection was performed as described in Varinelli *et al* at the Peritoneal Malignances Unit of IRCCS Foundation Istituto Nazionale dei Tumori di Milano[37] Briefly, non-tumoral tissues were collected 10 cm away from tumor, according to standard clinical procedures[30] Neoplastic-derived and normal-derived 3D decellularized extracellular matrix (3D-dECM) specimens were obtained as described in Genovese et al. [38]. 3D-dECM were embedded in OCT and then frozen in liquid nitrogen bath of isopropanol. Frozen samples were cut into slices of 100-200µm thickness and immobilized on polarized glass slides (Thermofisher, Walthan, USA). Prepared samples were stored at -4°C and used for the AFM measurements.

Table 1 Characteristics of the patients from whom the tissue samples were obtained.

Patient	**Age**[1]	**Oncogene Mutation**	**Sex**	**Diagnosis**[2]
CRC-PM 1[3)]	51	KRAS	Female	Mucinous Adenocarcinoma, stage IV
CRC-PM 2	47	NONE	Female	Adenocarcinoma of the sigma, stage IV
CRC-PM 3	40	NONE	Male	Adenocarcinoma, stage IV
CRC-PM 4	82	NONE	Female	Intestinal mucinous adenocarcinoma, stage IV
CRC-PM 5[3)]	66	BRAF	Female	Adenocarcinoma, stage IV
CRC-PM 6	71	KRAS	Female	Adenocarcinoma, stage IV
CRC-PM 7	47	BRAF	Male	Adenocarcinoma mucinous, stage IV
CRC-PM 8	43	KRAS	Male	Mucinous adenocarcinoma moderately differentiated, stage IV
CRC-PM 9[3)]	45	KRAS	Female	Intestinal mucinous adenocarcinoma
CRC-PM 10[3)]	63	KRAS	Male	Signet ring cell intestinal adenocarcinoma, stage IV
CRC-PM 11[3)]	67	KRAS	Male	Intestinal mucinous Adenocarcinoma , stage IV
CRC-PM 12	65	KRAS	Female	Adenocarcinoma of the sigma, stage IV
CRC-PM 13	81	#	Female	Well differentiated Intestinal Neuroendocrine tumor, NET G1, stage IV
CRC-PM 14	61	BRAF	Male	Adenocarcinoma, moderately differentiated stage IV

[1] Age of the patient on the day of the surgery.

[2] The stage of the cancer was determined according to the WHO classification [66].

[3] See Varinelli et al. 2022 [37].

AFM nanoindentation measurements

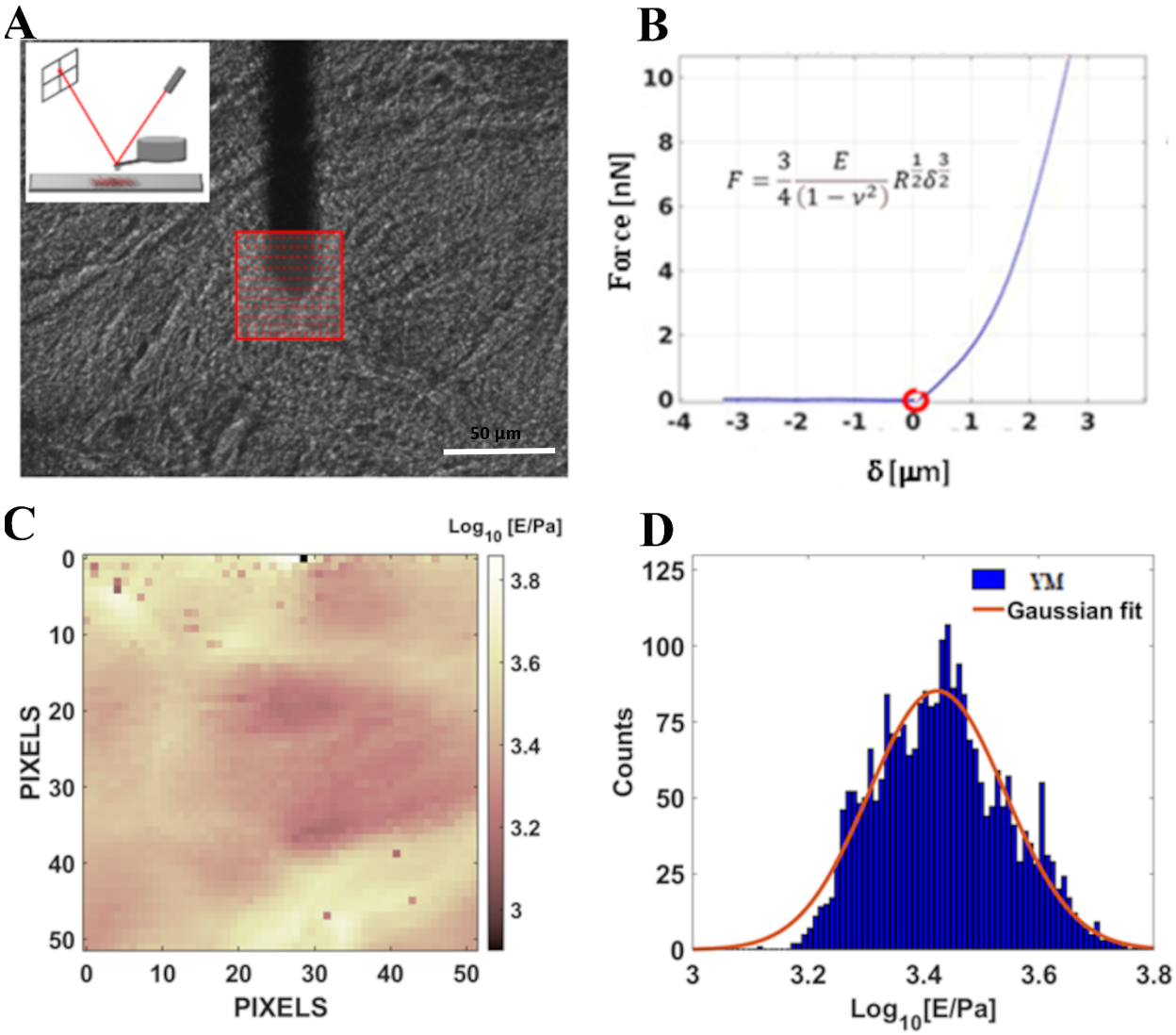

Figure 1. Schematic representation of the nanomechanical measurement. A) Optical image of a peritoneum ECM (normal-derived from patient 8), with the AFM cantilever and the selected region of interest for the indentation experiment. Slices with thickness between 100 and 200 µm are semi-transparent, which allows to select regions for the analysis that look sufficiently uniform and smooth. The red grid represents the locations where FCs are acquired (scale bar length – 50µm). In

the inset, the experimental setup for indentation measurements and the optical beam deflection system are shown. B) Typical rescaled approaching force vs indentation curve. The red circle highlights the contact point. Only the portion of the curve characterized by positive indentation is considered for the Hertzian fit (Eq. 1 and also shown in the inset). C) The map of Young's modulus values extracted by the FCs acquired in the region of interested shown in A. D) Histogram representing the distribution of YM values represented in the mechanical map in C. Under the hypothesis of a log-normal distribution, a Gaussian fit in semi-log scale allows to identify the median YM value, as the center of the Gaussian curve.

The nanomechanical measurements were performed using a Bioscope Catalyst AFM (Bruker) mounted on top of an inverted microscope optical microscope (Olympus X71). To isolate the AFM from ground and acoustic noise, the microscope was placed on an active antivibration base (DVIA-T45, Daeil Systems) inside an acoustic enclosure (Schaefer, Italy). AFM measurements of cryosections were performed in a PBS droplet confined by a circle of hydrophobic ink.

AFM-based nanomechanical measurements were performed according to standard procedures, as described in Refs [28,39]. The measurement process is described schematically in Figure 1. We have used custom colloidal probes with spherical tips made of borosilicate glass beads with diameter (twice the radius R) in the range 18-25µm, produced and calibrated as described in Ref. [40]. The spring constant of the AFM probes (typically 5-6 N/m) was calibrated using the thermal noise method [41,42]. The deflection sensitivity of the optical beam deflection apparatus (in units of nm/V) was calculated as the inverse of the slope of the force vs. distance curves (simply force curves, FCs) collected on a stiff substrate (the glass slide holding the sample)[39] or using the contactless SNAP procedure[43].

The samples were studied by collecting set of FCs, also called force volumes (FVs). Each FV typically covered an area between 50µm x 50µm to 125µm x125 µm and consisted of 100-225 FCs. The separation between adjacent FCs was chosen to be greater than the typical contact radius at maximum indentation, to reduce correlations between neighbouring FCs. For each patient's condition (normal or neoplastic), several FVs were collected on

different, macroscopically separated locations on each sample, with 2-3 samples (cryosections) per condition (normal vs neoplastic) for each patient. In total, for each condition 2000-4000 FCs were collected (Figure 1). A FC typically contained 8192 points, with ramp length L = 15 μm, maximum load F_{max} = 800 – 1500 nN, ramp frequency f = 1 Hz. The maximum load was adjusted to obtain a maximum indentation of 4-6 μm in all samples. Acquired data was analysed in MATLAB using protocol previously described in Puricelli et al.[28]. The elastic properties of the ECMs were characterized through their Young's modulus (YM) of elasticity, extracted by fitting the Hertz model [29,44] to the 20%-80% indentation range of the FCs (details in Ref. [26,28]):

$$F = \frac{4}{3}\frac{E}{1-\nu^2}R^{\frac{1}{2}}\delta^{\frac{3}{2}} \qquad (1)$$

which is accurate as long as the indentation δ is small compared to the radius R. In Eq. (1), ν is the Poisson's coefficient, which is typically assumed to be equal to 0.5 for in-compressible materials, and E is the YM.

Finite thickness correction [28,45–47] was not applied since the thickness of the ECM slices (150-200μm) is significantly larger than the expected contact radius at maximum indentation. The first 20% of the FCs is typically ignored, due to the contribution of superficial non- crosslinked fibers, surface roughness issues, etc.[12].

Histochemistry (HC) and immunofluorescence (IF) analyses

Before HC and IF staining, formalin-fixed-paraffin-embedded (FFPE) blocks were prepared and cut as in Varinelli *et al* [37]. FFPE sections were stained with haematoxylin and eosin (H&E) for quality control. For HC analysis, sections were stained with picrosirius red (ScyTek lab), to visualized collagen fibers, following the manufacturers' instructions. Antigen retrieval IF analysis was carried out as in Varinelli *et al* [37]. For IF analyses, FFPE sections were stained with primary alpha Smooth Muscle-FITC (1:400), FITC conjugated antibody (Merck, KGaA) and DAPI (Merck, KGaA), following the manufacturers' instructions. Images were acquired with a DM6000B microscope (Wetzlar, Germany Leica,) equipped with a 100 W mercury lamp, and analyzed using Cytovision software (Leica). All the experiments were performed in triplicate.

DNA sequencing

The principal mutational profile of PM patients (eg. KRAS and BRAF mutations) were determined by DNA sequencing. DNA from FFPE sections of PM patient's tissues was used for mutational analysis and extracted as in Varinelli *et al*[37]. About 150–200 ng genomic DNA (measured with Qubit dsDNA HS assay kit, ThermoFisher Scientific), were sheared by the Sure Select Enzymatic Fragmentation kit (Agilent Technologies Inc., Santa Clara, CA, USA). NGS libraries, the designer of probe set, the DNA sequencing and data analysis were performed as in Varinelli *et al* [37]. All the experiments were performed in triplicate.

Statistics

In order to evaluate the distribution of YM values that is peculiar of ECM in the different tested conditions, all values of the YM from all FCs have been pooled together. This is justified in part by the fact that curve to curve distance is of the order of the maximum contact radius, and also by the fact that separation between FVs from the same slice is comparable to the separation between FV from different slices obtained from the same patient. To show the YM distribution, violin plots have been used (Figure 2). The evaluation of representative YM values for a specific condition of a specific patient has been done by pooling the median YM values obtained from all FVs and calculating their mean value and the corresponding standard deviation of the mean, assuming that the median values should be normally distributed according to the central limit theorem [32,48]. Boxplots have been used to represent the distribution of median values (Figure 2). An experimental relative error of approximately 3%, evaluated using a Monte Carlo method[49], taking into account the uncertainties in the calibration factors (10% for the spring constant, 5% for the deflection sensitivity) was added in quadrature to the standard deviation of the mean to estimate the final error associated to the mean median YM values.

The statistical significance between tested conditions was assessed using a two-tailed t-test. In case of a p-value <0.05, the difference was considered as statistically significant.

Results

Changes in the nanomechanical properties of the ECM

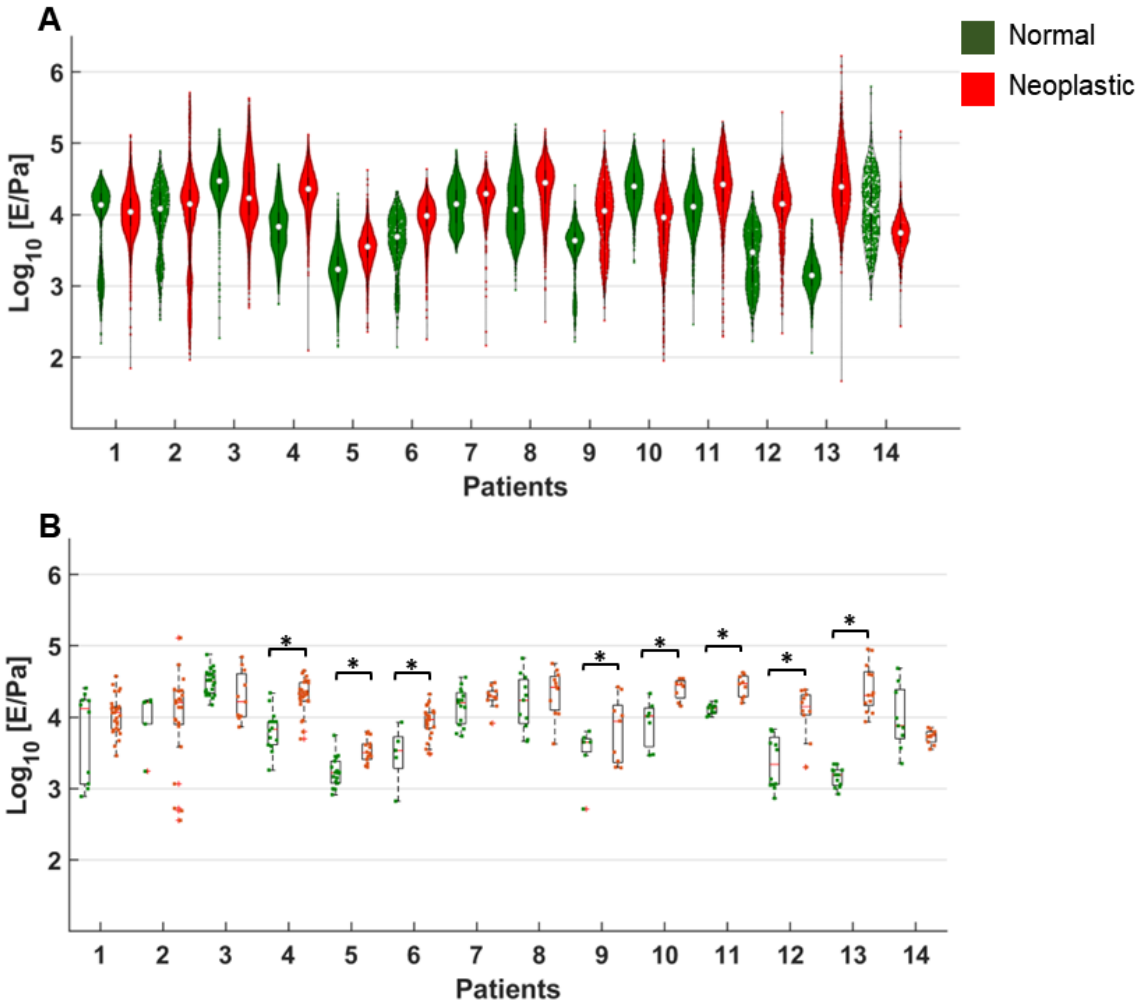

Figure 2. The graph presents the YM distributions for the normal (green) and neoplastic (red) conditions from human peritoneum ECMs for all patients considered in this study. A) Violin plots obtained by pooling all YM values from all FCs acquired for a specific condition. Median is represented by white dot and black thick lines are upper and lower quartile B) Box plots showing the distribution of median (red line) YM values from all FVs collected for a specific condition. Each square represents median value of single ROI measurement. The top and bottom edges of the boxes represent the upper and lower quartile. The whiskers (dotted line) extend to the nonoutlier maximum and minimum. The red '+' sign stands for outliers (values more than 1.5*IQR (interquartile range)).

Statistically significant stiffening (i.e. increase of the YM value from the normal to the neoplastic condition) of the ECM derived from patients affected by CRC -derived PM was observed in the case of patients 4,5,6 and 9 - 13, who were also among the oldest patients: 82, 66 and 71 years old, respectively, for patients 4-6 and 63, 67, for patients 10-13. However, the process of stiffening was present also in patients 7, 8 and 9, who are significantly younger (47, 43 and 45 years old) (Figure 1A).

For both normal and neoplastic conditions, the distribution of YM values are rather broad. Within the same condition, we observed very large patient to patient variability. For example, for the normal condition, we observed a factor of ~17 difference between the YM value of patients 5 and 3; for the neoplastic condition, we observed a factor of ~8 difference between the YM value of patients 8 and 5. These results highlight, among other aspects, the importance of identifying internal references within the same patient; in our case, this is represented by the normal ECM collected several centimeters away from the tumoral lesion.

The heterogeneity of the studied ECM samples can be appreciated from the violin plots shown in Figure 2A. In several cases, the YM distribution appear as clearly multimodal. It turns out that often the YM value of the highest-order mode is similar (i.e., the distribution shows significant overlap) to the YM value of a leading mode in the distribution of the neoplastic sample (see for example patients 1,2,3,6,7,8).

Figure 2B shows the distribution of the median YM values measured in different locations of the ECM samples for the tested conditions and patients. In some cases, stiffening is statistically significant, in others it is not, although an increase in the median value of the YM is often observed (Figure 2B).

αSMA overexpression correlates with tissue stiffness

Given the results shown in Figure 2, we selected 6 different cases (patients) with somewhat paradigmatic mechanical behaviour to better understand the biological events that have sustained the mechanical behaviour, we performed αSMA staining, which is a marker of CAF activity related to collagen deposition leading to an increase in ECM's stiffness and its remodelling.

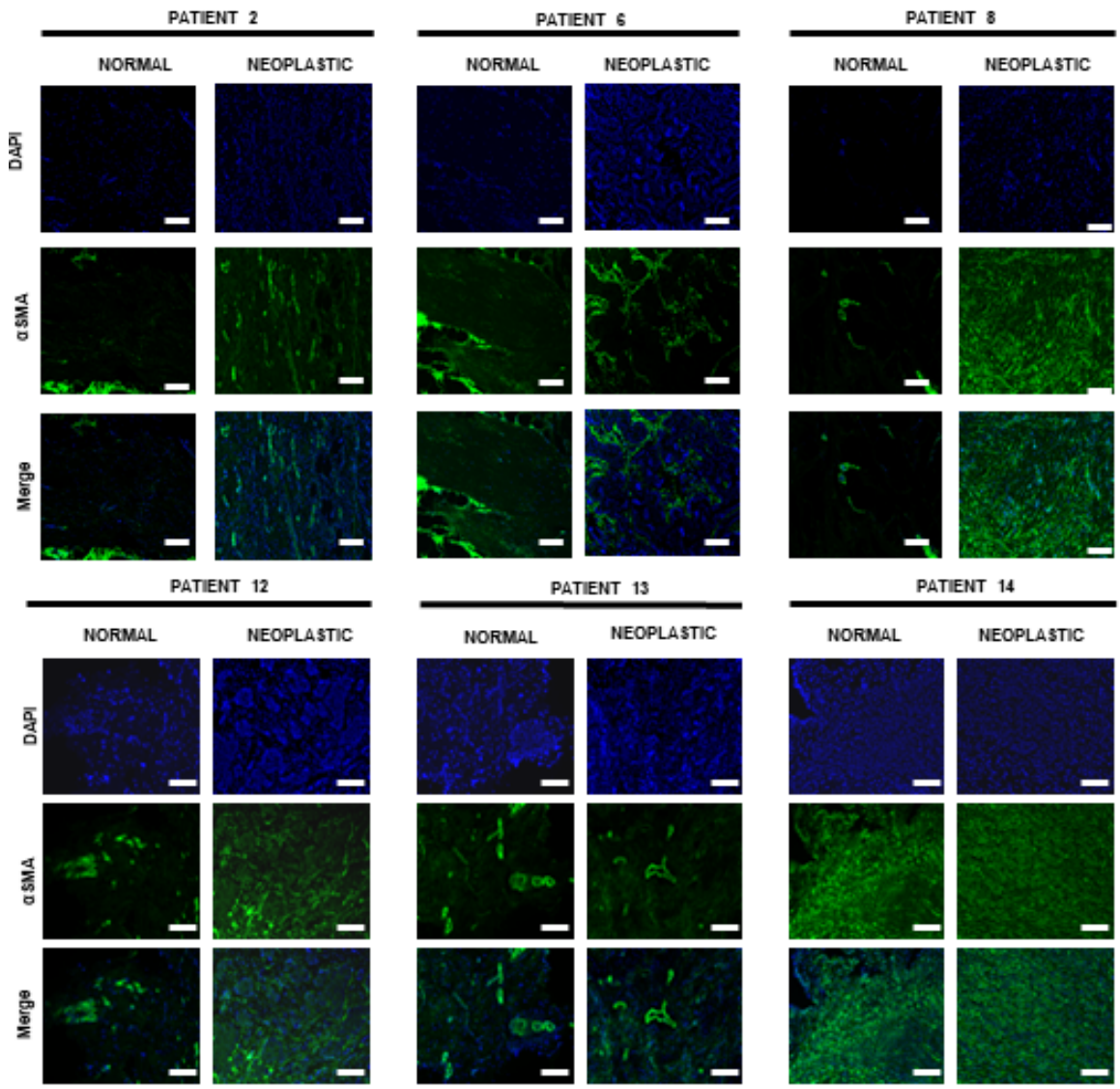

Figure 3. Images of tissue samples from patient 2, 6, 8 and 12-14 stained for visualization of cell nuclei (DAPI) and αSMA. Magnification is 10x.

The results showed a low expression of αSMA in normal-derived samples, although stromal-derived areas, characterized an overexpression of αSMA signal can be observed in patient 2, 6, 8 and 12, which is a sign of activity of CAF (Figure 3). Interestingly, we also observed higher expression of αSMA protein around blood vessels in normal-derived tissues (patients 6, 8 and 13), which is a sign of the neo-angiogenesis process, that is a well know hallmark of cancer and metastatic spread. On the other hand, neoplastic-derived samples showed an overexpression of

αSMA protein, although we could observe areas where αSMA expression is comparable to that of the normal tissues (Figure 3). Patient 14 showed a similar expression pattern in both normal and neoplastic-derived tissues, characterized by an overexpression of αSMA signal. Lower expression of αSMA correlates with lower YM values, what can be observed in case of normal-derived samples from patients 12 and 13 while in stiffer, tumor-derived samples of patient 12 and 8, overexpression of αSMA was on high level (Figure 2B and 3). Additionally, in patient 2, 8 (normal) and 12 (normal) stiffness distribution was bimodal (Figure 2A) and similar distribution can be observed for expression of αSMA protein. These observations link changes in ECM stiffness with expression of αSMA, thus activity of CAF during PM.

αSMA overexpression correlates with collagen fibres deposition and orientation

Next, we evaluated the orientation of the collagen fibers with Picrosirius Red staining (Figure 4). The results showed that normal samples have a greater collagen fibers deposition in the stromal and blood vessel areas, with random relative orientation (Figure 4, see patients 2, 6, 8), while neoplastic-derived samples were characterized by irregular and porous collagen fibers orientation, with a corrugated-like morphology pattern (Figure 4, see patients 2, 6, 8, 12, 13, 14). Overall, these results correlated with the expression of αSMA signal, suggesting the active role of CAF in collagen production and deposition during the metastatic spread (Figure 3 and 4, see patients 2, 6, 8 and 14). Moreover, we observed that some normal-derived samples presented a neoplastic-like collagen pattern, also in line with αSMA expression, especially for patient 14 (Figure 3 and 4, see patients 12, 13, 14).

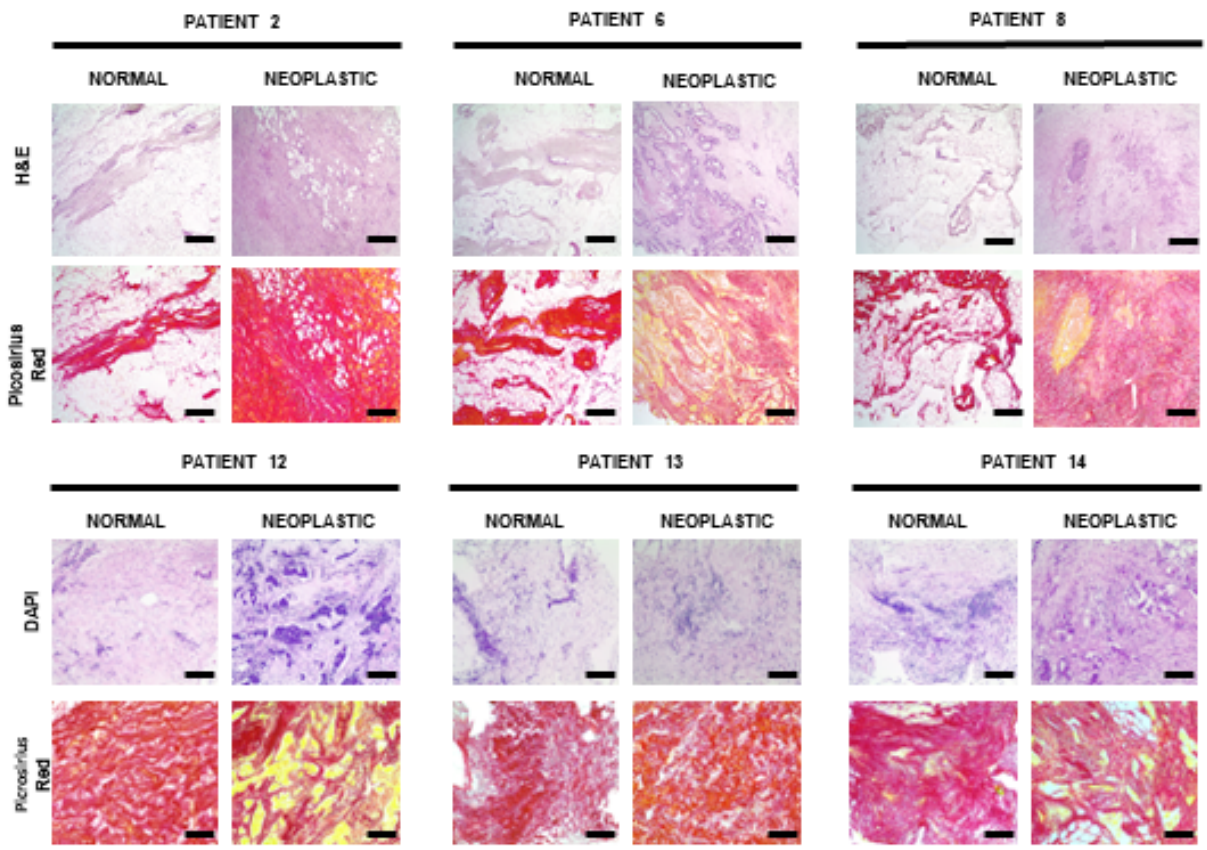

Figure 4. H&E and picrosirius Red staining of tissue samples from patients 2, 6, 8 and 12-14. Magnification 4x.

Correlation of the mechanical fingerprint with patients' clinical data

To further understand how the mechanical response and modifications of the ECM are related to PM, we looked for correlations between the observed biophysical properties and specific clinical data of the patients.

To this purpose, we first checked whether the Young's modulus of the normal ECM correlates with the age of the patients involved, since age-related stiffening at both cell and ECM/tissue level has been reported[50–54]. The results are shown in Figure 5A. It is possible to observe a clear trend that leads toward softening of the tissue for older patients. This result is quite counter intuitive, also considered the cited literature. We think that this opposite trend is due to damaging

and inflammation of the tissue due to previous chemotherapy treatments, a common feature of all patients considered in this study.

To avoid the previous treatments -related bias, we decided to focus the analysis on the relative stiffening of neoplastic vs normal ECMs within every single patient, since both normal and neoplastic tissues have experienced the same treatment. As it is shown in Figure 5B, no apparent correlation is present between the relative increase of stiffness and the patients' age. To be noted, patient 13 (highlighted with a triangular mark in the figures), who showed the strongest increase of stiffness (up to 1200%, and four times larger than the second highest relative stiffening), was not affected by CRC, but by a neuroendocrine colon cancer. The abnormal stiffening observed in patient 13, compared to the other patients, can be a sign of different mechanical modifications between tumor types. Nevertheless, since neuroendocrine cancer are extremely rare, our observations are not statistically significant and comparison with the case of CRC -derived PCs cannot be done; patient 13 has been ignored in the following correlation analysis.

Following clinical characterization of the tumor types, we checked whether the stiffening is correlated with the most common mutations of PM disease (Figure 5C). Interestingly, we observed a difference (even if not significant) between the relative stiffening of ECMs showing KRAS and BRAF mutations, while the non-mutated tumor seems to span a wider range of relative stiffening, encompassing those of the two mutations.

Eventually, we decided to look for correlations between the relative stiffening and the sex of the patients, since it is known that colorectal cancer is more frequent in males compared to females, but the differences in mortality seem to be irrelevant[55]. Figure 5D shows that a difference in the relative stiffening of the ECMs of male and female patients is present, females showing a more pronounced stiffening. It could be interesting to check for sex related changes in the mechanical properties of other tissues, like for cardiovascular diseases, which are known to affect males more than females[56].

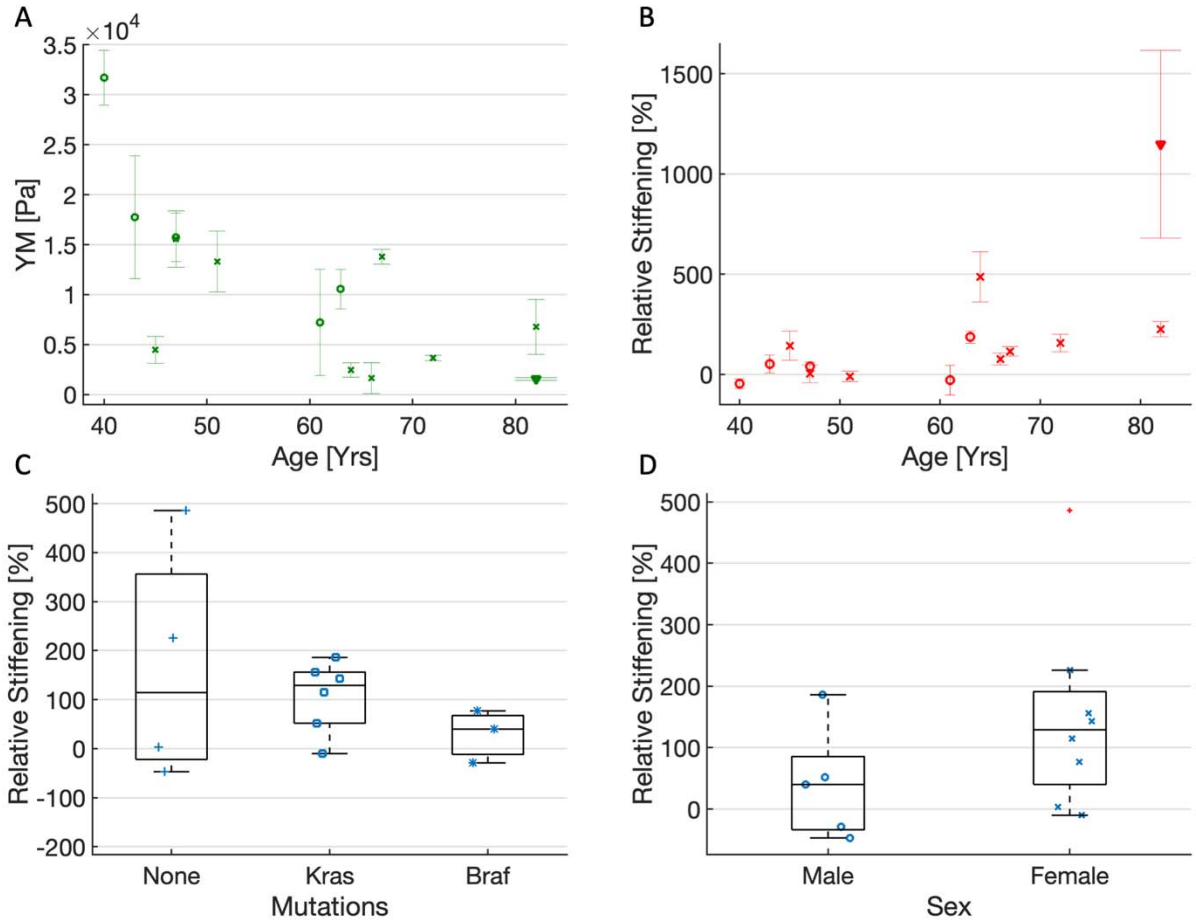

Figure 5. A) Absolute YM with STD of the mean coming from healthy ECM of the 14 patients as a function of their age (circles represents men patients while crosses represent female patients, triangle are different kind of colon-tumor). B) Relative stiffening of the neoplastic ECM compared to patients' age. C) Relative stiffening compared to transcription proteins mutations. D) Relative stiffening compared to patients' sex.

Discussion

Changes in nanomechanical properties of tissues are one of the hallmarks of tumor progression. By studying these changes and by better understanding the processes behind them, we could exploit this knowledge to implement early diagnosis of cancer and other diseases based on nano- and microscale mechanical phenotyping. Here, we focused on the investigation of the mechanical modifications in decellularized ECM derived from PM.

Based on AFM studies on ECM samples from 14 patients, we observed a general trend towards stiffening of the ECM during the development of the neoplastic lesion (Figure 1). Our results are in general agreement with previously published data on ECM [12,37]. The measured multimodal, not simply broad, distributions of YM values, suggest that the ECM possesses a significant structural, compositional, and therefore also mechanical heterogeneity at the scale of the AFM measurement, which is 10-100 µm. Moreover, the partial overlap of YM values distributions of different conditions (normal and neoplastic), revealed the complexity of the progression of the disease during the metastatic process, characterized by high spatial heterogeneity at the cellular and supracellular scale. The seed and soil theory suggests that ECM undergoes changes, including mechanical one, to prepare microenvironment suitable for neoplastic cells proliferation[57]. Observing stiffer regions in normal samples comparable to those typical of the neoplastic case suggested that local modifications preparing the ground for metastatic invasion in the normal tissue take place away from the existing lesion, likely caused by release of factors that can modify, at the end, the mechanical properties of the ECM[57]. Widespread practice for cancer related studies is to obtain non-tumor sample 10-15cm away from the tumor[30]. Our results suggest that for studying nanomechanical properties this distance may not be sufficient.

Staining of αSMA, a CAF-specific protein expressed in fibroblasts, which is a sign of cancer progression and typical marker of desmoplasia[22], detected modifications of the surrounding microenvironment that typically lead to the development of specific metastatic niches. Since we observed also in normal samples areas with high expression of αSMA, probably they could have undergone modification induced by specific pro-metasatic factors released by nearby PM metastatic cells. These results confirmed that formation of pre-metastatic niches occurs already in normal derived tissue, since we observed also in normal samples areas with high expression of αSMA.

Higher expression of αSMA was also observed in area rich in blood vessels (patients 6, 8 and 13). During metastasis, CAFs can be distributed through blood vessels to develop the so-called perivascular metastatic niches, able to sustain the activation of stromal cell in normal tissue via TGF-ß and pro-inflammatory and pleiotropic interleukin and cytokine secretion, which also contribute to initiate modifications in the ECM, including stiffening. Taken together, these

events generate a more suitable microenvironment to support metastatic spread and, in particular angiogenesis [22,23,57]. Expression of αSMA in vascularized areas indicates early steps of metastatic invasion in normal tissues.

αSMA was overexpressed in almost all neoplastic samples, nevertheless a few areas in some patients (2 and 6) exhibited a lower expression, which correlates with measured lower YM values in the neoplastic ECM (Figure 1)[23]. Based on these results we can conclude that part of the tissue that was assumed to be not tumorous was actually partially affected by developing tumour[30]. Another step to better understand the differences between normal and neoplastic ECM was to visualize collagen I and III fibers, as their overexpression and remodelling are strictly related to cancer progression[5–8,58]. Our results showed typical expression and organization of collagen fibers that was already observed in previous studies on different types of ECM[12,59]. Organization of collagen fibers was strictly correlated with expression of αSMA; expression of this protein confirmed collagen crosslinking in neoplastic ECM but also to a smaller extent in normal ECM. Tumors with high desmoplasia (fiber crosslinking) are considered to be more aggressive and associated with worse prognosis[5]. In the neoplastic samples, increased crosslinking and restructuring of collagen fibrils in the ECM, and matrix stiffening produce an extracellular environment that is favourable to tumor invasion and growth. Changes in the vascularized and stiffer perilesional area could be a feed-forward loop to spread neoplastic ECM characteristics. Myofibroblasts are known for their ECM remodelling, which involves de novo deposition of specific receptors involved in the mechanosignaling by the ECM, contributing to both normal and pathologic tissue remodelling[60].

Data obtained from the correlations between the observed biophysical properties and specific clinical data of the patients, suggest a clear trend that leads toward softening of the tissue for older patients. This result is quite counter intuitive, also considered that age-related stiffening at both cell and ECM/tissue level has been reported[50–54]. We think that this opposite trend is due to damaging and inflammation of the tissue due to previous chemotherapy treatments, a common feature of all patients considered in this study. For this reason, we decided to focus the analysis on the relative stiffening of neoplastic vs normal ECMs within every single patient, since both normal and neoplastic tissues have experienced the same treatment. On the other hand, the study of mechanical properties within the mutational profile, showed that patients carrying KRAS and

BRAF had a specific value of stiffness, while patients' wild type for those mutations had a much more variable stiffness. Since KRAS and BRAF are two of the most common mutations for PM, they probably seem to show specific and peculiar mechanical characteristics. This data is still preliminary and will be investigated with further experiments. Since it is known that CRC is more frequent in males compared to females, and the differences in mortality seem to be irrelevant[55]. We believe that such correlations would help to push forward the development of biomechanical tests that could be flanked by standard clinical diagnosis techniques.

Understanding how modifications of the mechanical properties of the ECM influence the metastatic invasion may also have a potential in developing active tissue treatments that can impact on the cell migration; ECM is being used already as a scaffold for cell culture to better understand the cell-microenvironment interaction mechanisms [7,37,61–65].

Conclusions

In this work we provided evidence that in the case of CRC-derived peritoneal metastasis, the stiffening of ECM is correlated to collagen deposition and remodelling and activity of CAF. Spatially resolved mechanical analysis of human-derived samples highlighted significant spatial heterogeneity of the elastic properties of both normal and neoplastic ECMs. These results, together with overexpression of αSMA, revealed that signs of forming pre-metastatic niche are already present in normal derived tissue, which gives a chance to use the nano- and microscale characterization of the mechanical properties of tissues as a cancer diagnosis tool. Finally, a better understanding of the ECM properties will facilitate using ECM as a scaffold for culturing cells in future research by creating more reliable models of the diseased tissue.

Acknowledgements

This research was funded by the European Union's Horizon 2020 research and innovation program under the Marie Skłodowska-Curie grant agreement No. 812772, project Phys2Biomed, and under FET Open grant agreement No. 801126, project EDIT. This work was supported by "5

per 1000" funds (2019 MUR and 2015 Ministry of Health, financial support for research) – institutional grant BRI 2021 "Harnessing the extracellular matrix to awaken the immune response in patients with peritoneal metastasis" assigned to Dr. Luca Varinelli, and by the Italian Ministry of Health, with a grant agreement No. RF2019-12370456. We thank the patients who participated in the study. We thank Hatice Holuigue for her valuable support and discussions.

Bibliography

[1] W. Ceelen, R.G. Ramsay, V. Narasimhan, A.G. Heriot, O. de Wever, Targeting the Tumor Microenvironment in Colorectal Peritoneal Metastases, Trends in Cancer. 6 (2020) 236–246. https://doi.org/10.1016/j.trecan.2019.12.008.

[2] D. Jayne, Molecular biology of peritoneal carcinomatosis, Cancer Treat Res. 134 (2007) 21–33. https://doi.org/10.1007/978-0-387-48993-3_2.

[3] L. Lemoine, P. Sugarbaker, K. van der Speeten, Pathophysiology of colorectal peritoneal carcinomatosis: Role of the peritoneum, World Journal of Gastroentology. 22 (2016) 7692–7707. https://doi.org/10.3748/wjg.v22.i34.7692.

[4] I. Jorba, J.J. Uriarte, N. Campillo, R. Farré, D. Navajas, Probing Micromechanical Properties of the Extracellular Matrix of Soft Tissues by Atomic Force Microscopy, Journal of Cellular Physiology. 232 (2017) 19–26. https://doi.org/10.1002/jcp.25420.

[5] S.S. Deville, N. Cordes, The Extracellular, Cellular, and Nuclear Stiffness, a Trinity in the Cancer Resistome—A Review, Frontiers in Oncology. 9 (2019) 1376. https://doi.org/10.3389/fonc.2019.01376. eCollection 2019.

[6] C. Frantz, K.M. Stewart, V.M. Weaver, The extracellular matrix at a glance, Journal of Cell Science. 123 (2010) 4195–4200. https://doi.org/10.1242/jcs.023820.

[7] P.K. Viji Babu, C. Rianna, U. Mirastschijski, M. Radmacher, Nano-mechanical mapping of interdependent cell and ECM mechanics by AFM force spectroscopy, Scientific Reports. 9 (2019) 12317. https://doi.org/10.1038/s41598-019-48566-7.

[8] P. Lu, V.M. Weaver, Z. Werb, The extracellular matrix: A dynamic niche in cancer progression, Journal of Cell Biology. 196 (2012) 395–406. https://doi.org/10.1083/jcb.201102147.

[9] M. Chighizola, A. Previdi, T. Dini, C. Piazzoni, C. Lenardi, P. Milani, C. Schulte, A. Podesta', Adhesion force spectroscopy with nanostructured colloidal probes reveals nanotopography-dependent early mechanotransductive interactions at the cell membrane level, BioRxiv. (2020) 2020.01.02.892919. https://doi.org/10.1101/2020.01.02.892919.

[10] M.A. Karsdal, M.J. Nielsen, J.M. Sand, K. Henriksen, F. Genovese, A.C. Bay-Jensen, V. Smith, J.I. Adamkewicz, C. Christiansen, D.J. Leeming, Extracellular matrix remodeling: The common

denominator in connective tissue diseases possibilities for evaluation and current understanding of the matrix as more than a passive architecture, but a key player in tissue failure, Assay and Drug Development Technologies. 11 (2013) 70–92. https://doi.org/10.1089/adt.2012.474.

[11] T.R. Cox, The matrix in cancer, Nature Reviews Cancer. 21 (2021) 217–238. https://doi.org/10.1038/s41568-020-00329-7.

[12] M. Nebuloni, L. Albarello, A. Andolfo, C. Magagnotti, L. Genovese, I. Locatelli, G. Tonon, E. Longhi, P. Zerbi, R. Allevi, A. Podestà, L. Puricelli, P. Milani, A. Soldarini, A. Salonia, M. Alfano, Insight On Colorectal Carcinoma Infiltration by Studying Perilesional Extracellular Matrix, Nature Publishing Group. (2016) 1–13. https://doi.org/10.1038/srep22522.

[13] M.J. Bissell, W.C. Hines, Why don't we get more cancer? A proposed role of the microenvironment in restraining cancer progression, Nature Medicine. 17 (2011) 320–329. https://doi.org/10.1038/nm.2328.

[14] J. Winkler, A. Abisoye-Ogunniyan, K.J. Metcalf, Z. Werb, Concepts of extracellular matrix remodelling in tumour progression and metastasis, Nature Communications. 11 (2020) 5120. https://doi.org/10.1038/s41467-020-18794-x.

[15] J. Alcaraz, J. Otero, I. Jorba, D. Navajas, Bidirectional mechanobiology between cells and their local extracellular matrix probed by atomic force microscopy, Seminars in Cell and Developmental Biology. 73 (2018) 71–81. https://doi.org/10.1016/j.semcdb.2017.07.020.

[16] A.M. Handorf, Y. Zhou, M.A. Halanski, W.J. Li, Tissue stiffness dictates development, homeostasis, and disease progression, Organogenesis. 11 (2015) 1–15. https://doi.org/10.1080/15476278.2015.1019687.

[17] M. Giussani, E. Landoni, G. Merlino, F. Turdo, S. Veneroni, B. Paolini, V. Cappelletti, R. Miceli, R. Orlandi, T. Triulzi, E. Tagliabue, Extracellular matrix proteins as diagnostic markers of breast carcinoma, Journal of Cellular Physiology. 233 (2018) 6280–6290. https://doi.org/10.1002/jcp.26513.

[18] M. Plodinec, M. Loparic, C.A. Monnier, E.C. Obermann, R. Zanetti-Dallenbach, P. Oertle, J.T. Hyotyla, U. Aebi, M. Bentires-Alj, R.Y.H. Lim, C.-A. Schoenenberger, The nanomechanical signature of breast cancer, Nature Nanotechnology. 7 (2012) 757–765. https://doi.org/10.1038/nnano.2012.167.

[19] K.R. Levental, H. Yu, L. Kass, J.N. Lakins, M. Egeblad, J.T. Erler, S.F.T. Fong, K. Csiszar, A. Giaccia, W. Weninger, M. Yamauchi, D.L. Gasser, V.M. Weaver, Matrix Crosslinking Forces Tumor Progression by Enhancing Integrin Signaling, Cell. 139 (2009) 891–906. https://doi.org/10.1016/j.cell.2009.10.027.

[20] D.T. Butcher, T. Alliston, V.M. Weaver, A tense situation: Forcing tumour progression, Nature Reviews Cancer. 9 (2009) 108–122. https://doi.org/10.1038/nrc2544.

[21] M. Hunter Joyce, C. Lu, E.R. James, R. Hegab, S.C. Allen, L.J. Suggs, A. Brock, Phenotypic basis for matrix stiffness-dependent chemoresistance of breast cancer cells to doxorubicin, Frontiers in Oncology. 8 (2018) 337. https://doi.org/10.3389/fonc.2018.00337.

[22] R.-P. Czekay, D.-J. Cheon, R. Samarakoon, S.M. Kutz, P.J. Higgins, Cancer-Associated Fibroblasts: Mechanisms of Tumor Progression and Novel Therapeutic Targets, Cancers (Basel). 14 (2022) 1231. https://doi.org/10.3390/cancers14051231.

[23] P. Chiarugi, P. Cirri, Cancer associated fibroblasts: the dark side of the coin, American Journal of Cancer Research. 1 (2011) 482–497.

[24] M. Nurmik, P. Ullmann, F. Rodriguez, S. Haan, E. Letellier, In search of definitions: Cancer-associated fibroblasts and their markers, International Journal of Cancer. 146 (2020) 895–905. https://doi.org/10.1002/ijc.32193.

[25] A. Alessandrini, P. Facci, AFM: A versatile tool in biophysics, Measurement Science and Technology. 16 (2005). https://doi.org/10.1088/0957-0233/16/6/R01.

[26] H. Holuigue, E. Lorenc, M. Chighizola, C. Schulte, L. Varinelli, M. Deraco, M. Guaglio, M. Gariboldi, A. Podestà, Force Sensing on Cells and Tissues by Atomic Force Microscopy, Sensors. 22 (2022) 2197. https://doi.org/10.3390/s22062197.

[27] N. Gavara, A beginner's guide to atomic force microscopy probing for cell mechanics, Microscopy Research and Technique. 80 (2017) 75–84. https://doi.org/10.1002/jemt.22776.

[28] L. Puricelli, M. Galluzzi, C. Schulte, A. Podestà, P. Milani, Nanomechanical and topographical imaging of living cells by atomic force microscopy with colloidal probes, Review of Scientific Instruments. 86 (2015). https://doi.org/10.1063/1.4915896.

[29] S.-V. Kontomaris, The Hertz Model in AFM Nanoindentation Experiments: Applications in Biological Samples and Biomaterials, Micro and Nanosystems. 10 (2018) 11–22. https://doi.org/10.2174/1876402910666180426114700.

[30] P. Deptuła, D. Łysik, K. Pogoda, M. Cieśluk, A. Namiot, J. Mystkowska, G. Król, S. Głuszek, P.A. Janmey, R. Bucki, Tissue Rheology as a Possible Complementary Procedure to Advance Histological Diagnosis of Colon Cancer, ACS Biomaterials Science and Engineering. 6 (2020) 5620–5631. https://doi.org/10.1021/acsbiomaterials.0c00975.

[31] I. Jorba, G. Beltrán, B. Falcones, B. Suki, R. Farré, J.M. García-Aznar, D. Navajas, Nonlinear elasticity of the lung extracellular microenvironment is regulated by macroscale tissue strain, Acta Biomaterialia. 92 (2019) 265–276. https://doi.org/10.1016/j.actbio.2019.05.023.

[32] E. Shimshoni, I. Adir, R. Afik, I. Solomonov, A. Shenoy, M. Adler, L. Puricelli, F. Sabino, S. Savickas, O. Mouhadeb, N. Gluck, S. Fishman, L. Werner, T.M. Salame, D.S. Shouval, C. Varol, U. auf dem Keller, A. Podestà, T. Geiger, P. Milani, U. Alon, I. Sagi, Distinct extracellular–matrix remodeling events precede symptoms of inflammation, Matrix Biology. 96 (2021) 47–68. https://doi.org/10.1016/j.matbio.2020.11.001.

[33] M. Alfano, M. Nebuloni, R. Allevi, P. Zerbi, E. Longhi, R. Lucianò, I. Locatelli, A. Pecoraro, M. Indrieri, C. Speziali, C. Doglioni, P. Milani, F. Montorsi, A. Salonia, Linearized texture of three-dimensional extracellular matrix is mandatory for bladder cancer cell invasion, Scientific Reports. 6 (2016) 1–12. https://doi.org/10.1038/srep36128.

[34] M. Plodinec, R.Y.H. Lim, Nanomechanical characterization of living mammary tissues by atomic force microscopy, Methods in Molecular Biology. 1293 (2015) 231–246. https://doi.org/10.1007/978-1-4939-2519-3_14.

[35] A. Stylianou, M. Lekka, T. Stylianopoulos, AFM assessing of nanomechanical fingerprints for cancer early diagnosis and classification: From single cell to tissue level, Nanoscale. 10 (2018) 20930–20945. https://doi.org/10.1039/c8nr06146g.

[36] A. Stylianou, M. Lekka, T. Stylianopoulos, AFM assessing of nanomechanical fingerprints for cancer early diagnosis and classification: From single cell to tissue level, Nanoscale. 10 (2018) 20930–20945. https://doi.org/10.1039/c8nr06146g.

[37] L. Varinelli, M. Guaglio, S. Brich, S. Zanutto, A. Belfiore, F. Zanardi, F. Iannelli, A. Oldani, E. Costa, M. Chighizola, E. Lorenc, S.P. Minardi, S. Fortuzzi, M. Filugelli, G. Garzone, F. Pisati, M. Vecchi, G. Pruneri, K. Shigeki, D. Baratti, L. Cattaneo, D. Parazzoli, A. Podestà, M. Milione, M. Dearco, M.A. Pierotti, M. Gariboldi, Decellularized Normal and Tumor Extracellular Matrix as Scaffold for Cancer Organoid Cultures of Colorectal Peritoneal Metastases, 2022. https://doi.org/10.1101/2021.07.15.452437.

[38] L. Genovese, L. Zawada, A. Tosoni, A. Ferri, P. Zerbi, R. Allevi, M. Nebuloni, M. Alfano, Cellular localization, invasion, and turnover are differently influenced by healthy and tumor-derived extracellular matrix, Tissue Engineering - Part A. 20 (2014) 2005–2018. https://doi.org/10.1089/ten.tea.2013.0588.

[39] H.J. Butt, B. Cappella, M. Kappl, Force measurements with the atomic force microscope: Technique, interpretation and applications, Surface Science Reports. 59 (2005) 1–152. https://doi.org/10.1016/j.surfrep.2005.08.003.

[40] M. Indrieri, A. Podestà, G. Bongiorno, D. Marchesi, P. Milani, Adhesive-free colloidal probes for nanoscale force measurements: Production and characterization, Review of Scientific Instruments. 82 (2011) 023708. https://doi.org/10.1063/1.3553499.

[41] H.J. Butt, M. Jaschke, Calculation of thermal noise in atomic force microscopy, Nanotechnology. 6 (1995) 1–7. https://doi.org/10.1088/0957-4484/6/1/001.

[42] M. Chighizola, L. Puricelli, L. Bellon, A. Podestà, Large colloidal probes for atomic force microscopy: Fabrication and calibration issues, Journal of Molecular Recognition. 34 (2021) e2879. https://doi.org/10.1002/jmr.2879.

[43] H. Schillers, C. Rianna, J. Schäpe, T. Luque, H. Doschke, M. Wälte, J.J. Uriarte, N. Campillo, G.P.A. Michanetzis, J. Bobrowska, A. Dumitru, E.T. Herruzo, S. Bovio, P. Parot, M. Galluzzi, A. Podestà, L. Puricelli, S. Scheuring, Y. Missirlis, R. Garcia, M. Odorico, J.-M. Teulon, F. Lafont, M. Lekka, F. Rico, A. Rigato, J.-L. Pellequer, H. Oberleithner, D. Navajas, M. Radmacher, Standardized Nanomechanical Atomic Force Microscopy Procedure (SNAP) for Measuring Soft and Biological Samples, Scientific Reports. 7 (2017) 5117. https://doi.org/10.1038/s41598-017-05383-0.

[44] H. Hertz, Ueber die Berührung fester elastischer Körper, Journal Fur Die Reine Und Angewandte Mathematik. 1881 (1881) 156–171. https://doi.org/10.1515/crll.1882.92.156.

[45] E.K. Dimitriadis, F. Horkay, J. Maresca, B. Kachar, R.S. Chadwick, Determination of elastic moduli of thin layers of soft material using the atomic force microscope, Biophysical Journal. 82 (2002) 2798–2810. https://doi.org/10.1016/S0006-3495(02)75620-8.

[46] P.D. Garcia, R. Garcia, Determination of the Elastic Moduli of a Single Cell Cultured on a Rigid Support by Force Microscopy, Biophysical Journal. 114 (2018) 2923–2932. https://doi.org/10.1016/j.bpj.2018.05.012.

[47] N. Gavara, R.S. Chadwick, Determination of the elastic moduli of thin samples and adherent cells using conical atomic force microscope tips, Nature Nanotechnology. 7 (2012) 733–736. https://doi.org/10.1038/nnano.2012.163.

[48] H. Cramér, Mathematical Methods of Statistics, Princeton University Press, 1999.

[49] J.S. Alper, R.I. Gelb, Standard errors and confidence intervals in nonlinear regression: Comparison of Monte Carlo and parametric statistics, 1990. https://doi.org/10.1021/j100374a068.

[50] S.C. Lieber, N. Aubry, J. Pain, G. Diaz, S.J. Kim, S.F. Vatner, Aging increases stiffness of cardiac myocytes measured by atomic force microscopy nanoindentation, American Journal of Physiology - Heart and Circulatory Physiology. 287 (2004). https://doi.org/10.1152/ajpheart.00564.2003.

[51] J.C. Kohn, M.C. Lampi, C.A. Reinhart-King, Age-related vascular stiffening: Causes and consequences, Frontiers in Genetics. 6 (2015) 112. https://doi.org/10.3389/FGENE.2015.00112/BIBTEX.

[52] T.K. Arthroplasty, B.M. Index, C. Schulze, F. Wetzel, T. Kueper, A. Malsen, G. Muhr, S. Jaspers, T. Blatt, K.P. Wittern, H. Wenck, J.A. Käs, Stiffening of human skin fibroblasts with age, Biophysical Journal. 99 (2010) 2434–2442. https://doi.org/10.1016/j.bpj.2010.08.026.

[53] T.K. Berdyyeva, C.D. Woodworth, I. Sokolov, Human epithelial cells increase their rigidity with ageing in vitro: Direct measurements, Physics in Medicine and Biology. 50 (2005) 81–92. https://doi.org/10.1088/0031-9155/50/1/007.

[54] J. Huynh, N. Nishimura, K. Rana, J.M. Peloquin, J.P. Califano, C.R. Montague, M.R. King, C.B. Schaffer, C.A. Reinhart-King, Age-related intimal stiffening enhances endothelial permeability and leukocyte transmigration, Science Translational Medicine. 3 (2011). https://doi.org/10.1126/scitranslmed.3002761.

[55] A. White, L. Ironmonger, R.J.C. Steele, N. Ormiston-Smith, C. Crawford, A. Seims, A review of sex-related differences in colorectal cancer incidence, screening uptake, routes to diagnosis, cancer stage and survival in the UK, BMC Cancer. 18 (2018) 1–11. https://doi.org/10.1186/S12885-018-4786-7/TABLES/7.

[56] L. Mosca, E. Barrett-Connor, N. Kass Wenger, Sex/gender differences in cardiovascular disease prevention: What a difference a decade makes, Circulation. 124 (2011) 2145–2154. https://doi.org/10.1161/CIRCULATIONAHA.110.968792.

[57] M. Akhtar, A. Haider, S. Rashid, A.D.M.H. Al-Nabet, Paget's "Seed and Soil" Theory of Cancer Metastasis, Advances In Anatomic Pathology. 26 (2019) 69–74.

[58] M. Najafi, B. Farhood, K. Mortezaee, Extracellular matrix (ECM) stiffness and degradation as cancer drivers, Journal of Cellular Biochemistry. 120 (2019) 2782–2790. https://doi.org/10.1002/jcb.27681.

[59] O. Chaudhuri, S.T. Koshy, C. Branco Da Cunha, J.W. Shin, C.S. Verbeke, K.H. Allison, D.J. Mooney, Extracellular matrix stiffness and composition jointly regulate the induction of malignant phenotypes in mammary epithelium, Nature Materials. 13 (2014) 970–978. https://doi.org/10.1038/nmat4009.

[60] B. Ri Seo, X. Chen, L. Ling, Y. Hye Song, A.A. Shimpi, S. Choi, J. Gonzalez, J. Sapudom, K. Wang, R. Carlos Andresen Eguiluz, D. Gourdon, V.B. Shenoy, C. Fischbach, Collagen microarchitecture mechanically controls myofibroblast differentiation, Proceedings of the National Academy of Sciences of the United States of America. 117 (2020) 11387–11398. https://doi.org/10.1073/pnas.1919394117/-/DCSupplemental.

[61] L.P. Ferreira, V.M. Gaspar, J.F. Mano, Decellularized Extracellular Matrix for Bioengineering Physiomimetic 3D in Vitro Tumor Models, Trends in Biotechnology. 38 (2020) 1397–1414. https://doi.org/10.1016/j.tibtech.2020.04.006.

[62] F. Sensi, E. D'Angelo, S. D'Aronco, R. Molinaro, M. Agostini, Preclinical three-dimensional colorectal cancer model: The next generation of in vitro drug efficacy evaluation, Journal of Cellular Physiology. 234 (2018) 181–191. https://doi.org/10.1002/jcp.26812.

[63] Y. Miyauchi, K. Yasuchika, K. Fukumitsu, T. Ishii, S. Ogiso, T. Minami, H. Kojima, R. Yamaoka, H. Katayama, T. Kawai, E.Y. Yoshitoshi-Uebayashi, S. Kita, K. Yasuda, N. Sasaki, S. Uemoto, A novel three-dimensional culture system maintaining the physiological extracellular matrix of fibrotic model livers accelerates progression of hepatocellular carcinoma cells, Scientific Reports. 7 (2017) 9827. https://doi.org/10.1038/s41598-017-09391-y.

[64] J.F.E. Grey, A. Campbell-Ritchie, N.M. Everitt, A.J. Fezovich, S.P. Wheatley, The use of decellularised animal tissue to study disseminating cancer cells, Journal of Cell Science. 132 (2019). https://doi.org/10.1242/jcs.219907.

[65] D.K. Mishra, R.A. Miller, K.A. Pence, M.P. Kim, Small cell and non small cell lung cancer form metastasis on cellular 4D lung model, BMC Cancer. 18 (2018). https://doi.org/10.1186/s12885-018-4358-x.

[66] I. Ubink, W.J. van Eden, P. Snaebjornsson, N.F.M. Kok, J. van Kuik, W.M.U. van Grevenstein, M.M. Laclé, J. Sanders, R.J.A. Fijneman, S.G. Elias, I.H.M. Borel Rinkes, A.G.J. Aalbers, O. Kranenburg, Histopathological and molecular classification of colorectal cancer and corresponding peritoneal metastases, British Journal of Surgery. 105 (2018) 204–211. https://doi.org/10.1002/bjs.10788.